Concerted proton–electron transfers in the oxidation of phenols

Cyrille Costentin, Marc Robert and Jean-Michel Savéant*

Received 30th March 2010, Accepted 27th April 2010
DOI: 10.1039/c0cp00063a

The oxidation of phenols is an emblematic example where the mechanisms of proton-coupled electron transfers could be investigated in depth thanks to non-destructive electrochemical techniques such as cyclic voltammetry. A concerted proton–electron transfer could then be shown to be the prevailing pathway in the oxidation of amino-phenols mimicking the tyrosine–histidine couple in Photosystem II. The theoretical model developed on this occasion leads to the introduction of two main parameters characterizing reorganization of heavy atoms in the reactant and in the solvent on the one hand and proton tunneling on the other. When water used as the solvent is at the same time the proton acceptor, the concerted pathway also predominates. It is characterized by a remarkably large standard rate constant both in electrochemistry and in the oxidation by homogenous reactants. Another aspect of the importance of H-bonding in concerted proton–electron transfer is provided by H-bond relays that efficiently mediate the electron transfer-triggered transport of protons between two sites over large distances thanks to the displacement of two protons concerted with electron transfer. Intermediary protonation of the relay is avoided by fine tuning of its H-bond acceptor and donor properties.

1. Introduction

Oxidation of phenols currently attracts considerable attention for several reasons. One is connected to the role played by tyrosine in Photosystem II,[1–4] summarized in Scheme 1 as well as in other biological systems. [5] Other biological roles are also notable, such as their antioxidant properties.[6–8] Oxidative dehydrodimerization of phenols is also an important class of reactions, being involved in the first stages of natural processes such as lignin formation.[9,10] In addition, oxidation of phenols has noteworthy synthetic applications.[11]

Oxidation of phenols produces, after exchange of one electron and one proton, a neutral radical that may or may not dimerize according to the substituents on the phenyl ring. The mechanisms and kinetics of this proton-coupled electron transfer (PCET), in the case where proton and electron transfers involve different molecular centers, currently attract active attention as fundamental problems of chemical reactivity, related to the already-mentioned involvement of PCET in many natural processes.

In the PCET reactions discussed in the following, proton and electron transfers involve different centers unlike what happens in hydrogen-atom transfers. The reaction may go

Laboratoire d'Electrochimie Moléculaire, Unité Mixte de Recherche Université-CNRS No 7591, Université Paris Diderot, Bâtiment Lavoisier, 15 rue Jean de Baïf, 75205 Paris Cedex 13, France. E-mail: saveant@univ-paris-diderot.fr

Cyrille Costentin

Cyrille Costentin was born in Normandy, France in 1972. He received his undergraduate education at Ecole Normale Supérieure (Cachan, France) and pursued graduate studies with Prof. Jean-Michel Savéant and Dr Philippe Hapiot at the University of Paris-Diderot, receiving his PhD in 2000. After one year as a postdoctoral fellow at the University of Rochester, with Prof. J. P. Dinnocenzo, he joined the University of Paris-Diderot as associate professor. He was promoted to professor in 2007. His interests include mechanisms and reactivity in electron transfer chemistry with emphasis on electrochemical and theoretical approaches to proton-coupled electron transfer.

Marc Robert

Marc Robert was educated at the Ecole Normale Supérieure (Cachan, France) and gained his PhD in 1995 from Paris-Diderot University with Claude Andrieux and Jean-Michel Savéant, working on electron transfer chemistry. After one year as a postdoctoral fellow at Ohio State University with Matt Platz, he joined Paris-Diderot as associate professor. He was promoted to professor in 2004 and became a junior fellow of the University Institute of France in 2007. His interests include electrochemical, photochemical and theoretical approaches to electron transfer reactions, and proton-coupled electron transfer in both organic chemistry and biochemistry.

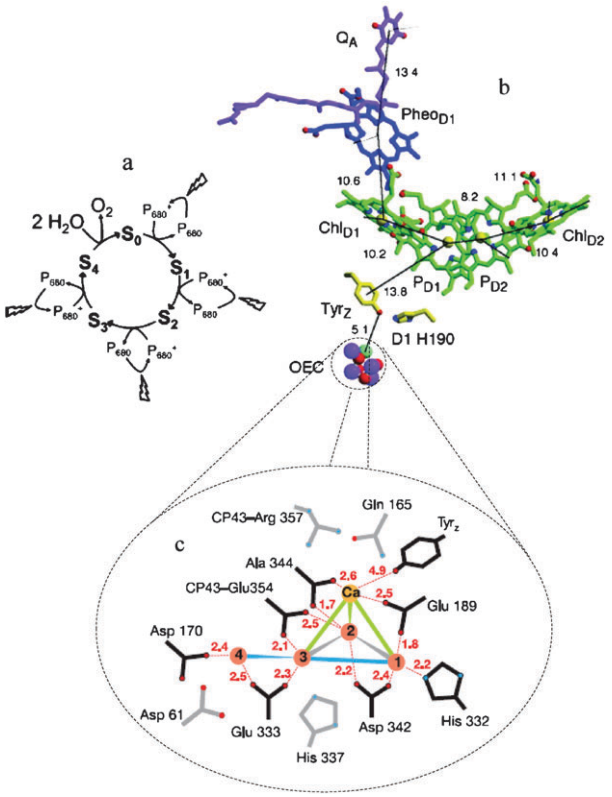

Scheme 1 Schematic view of Photosystem II. (a) Kok cycle.[13] (b) Structure of the reaction center of Photosystem II showing the TyrZ-ChlD1(P680)-PheoD1-QA donor–chromophore–acceptor system, electron transfer from tyrosine (TyrZ) being coupled to proton transfer from histidine D1 H190 (the numbers are the distances in angstroms). OEC, oxygen evolving complex.[14] (c) One proposed schematic view of the OEC Mn_4Ca[15] Ala, alanine; Arg, arginine; Asp, aspartate; Glu, glutamate; His, histidine. The numbers are the distances in angstroms. In the labeling scheme, amino acids in black are in the first coordination sphere and those beyond are in gray.

through an electron or proton transfer intermediate, giving rise to an EPT and a PET pathway, respectively (Scheme 2).

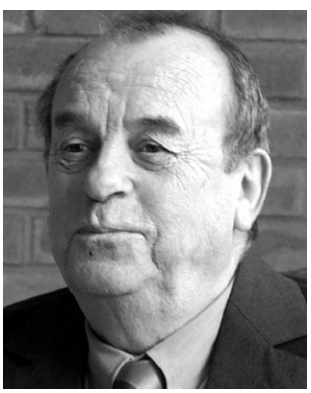

Jean-Michel Savéant

Jean-Michel Savéant was educated at the Ecole Normale Supérieure in Paris, and became the Vice-Director of the Chemistry Department before moving to the University Denis Diderot in 1971 where, from 1985, he was Directeur de Recherche. From 1988–89 he was a distinguished Fairchild Scholar at the California Institute of Technology. His current research involves all aspects of molecular and biomolecular electrochemistry as well as mechanisms and reactivity in electron transfer chemistry and biochemistry. He is a member of the French Academy of Sciences and foreign associate of the National Academy of Sciences of the USA.

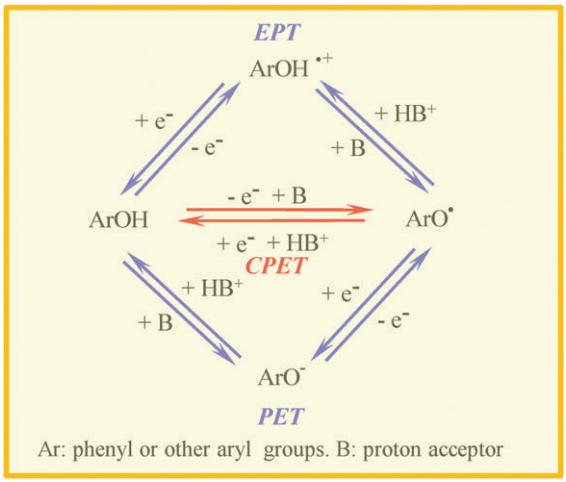

Scheme 2 PCET oxidation of phenols. Stepwise (blue) and concerted (red) pathways. EPT: electron transfer followed by proton transfer. PET: proton transfer followed by electron transfer. CPET: concerted proton–electron transfer.

In the "CPET" pathway, proton and electron transfers are concerted,[12] thus constituting a single elementary step.

The electrochemical approach of PCET oxidation of phenols has several advantages over other methodologies. Separation of the electron transfer (the electrode) and proton transfer sites, required to distinguished CPET reactions from H-atom transfers, is indeed readily achieved. In addition, changing the electrode potential is an easy way of varying the driving force of the reaction and the current is an on-line measure of the reaction kinetics. It follows that current–potential responses in non-destructive techniques like cyclic voltammetry may be read as a rate (from the current) driving force (from the electrode potential) relationship, provided the contribution of reactant transport has been duly taken into account (mainly diffusion). Intrinsic properties (properties at zero driving force) are therefore a natural outcome of the electrochemical approach. This approach will therefore be privileged in the following, although comparison with data pertaining to homogeneous oxidation will be made when available.

Concerted pathways have the advantage of by-passing the high-energy intermediates involved in the stepwise pathways—here the phenol cation radical on the one hand and the phenoxide ion on the other—even though this thermodynamic benefit may have a kinetic cost. The main task of mechanism analysis is, therefore, to distinguish the three pathways and to establish what are the factors that govern the competition between these pathways. Since mechanism determination is based on kinetics, it is helpful to have at one's disposal models leading to rate-driving force laws for all electron transfer steps including the CPET reaction. In the EPT pathway as well as in the PET pathway, electron transfers are of the outersphere type and one may therefore rely on the Marcus–Hush–Levich[16–19] model and the ensuing rate law, whereas the proton transfer steps may generally be considered as being so rapid as to remain at equilibrium.[20] This is not the case for the concerted pathway, where new models had to be devised for electrochemical and homogeneous CPET reactions[21–23] based on ideas originally developed for proton transfer.[24] More or less

sophisticated models have been elaborated on these bases but the large number of parameters involved and the uncertainty of quantum chemical calculations they may have to resort to make necessary a semi-empirical approach in which experimental tests are essential.

In the following sections, we describe typical electrochemical oxidations of phenols in which the occurrence of a concerted pathway has been ascertained in competition with the stepwise pathways.

The first example concern phenols that bear, attached to the structure, an amine serving as proton acceptor in the reaction mimicking the role of histidine 190 in the oxidation of tyrosine$_z$ in Photosystem II. It will introduce elements of theory that allow analysis of the kinetics of the CPET reaction in terms of rate law, reorganization energy and proton tunneling characteristics. The homogeneous oxidation of a similar molecule can also be compared with the electrochemical reaction. In the same section, oxidation of a hydroquinone bearing carboxylate groups in *ortho* positions will show that carboxylate groups, also ubiquitous in natural systems, could play a role similar to that of amines in the CPET oxidation of phenols. Investigation of water (with water as the solvent) as the proton acceptor is obviously of primary importance. This will be the subject of the next section, in which comparison with the oxidation of phenol by homogeneous one-electron oxidants will also be made. The remarkably high intrinsic reactivity thus observed requires further investigation of several leads. One of those is related to the Grotthuss mechanism of proton transport in water using the H-bonded and H-bonding character of water molecules in water. In this connection we describe in the next section the oxidation of a phenol molecule bearing an OH moiety in between the phenol functional group and the proton-accepting amine, which serves as proton transfer relay in the Grotthuss sense, *i.e.*, is not protonated during the course of the proton-coupled electron transfer process.

2. Oxidation of phenols with an attached proton acceptor

2.1 Phenols with an attached amine as proton acceptor

Phenols bearing an amine group located so as to form an H-bond with the phenol hydrogen of the type shown in Scheme 3 were synthesized as mimics of the tyrosine$_z$-histidine 190 system in Photosystem II (Scheme 1).[25] The main characteristics of their electrochemical oxidation[22,26] are summarized in Fig. 1. Cyclic voltammetry in acetonitrile (Fig. 1) shows a reversible wave corresponding to the one-electron–one-proton reversible conversion from the phenol–amine system to the phenoxyl radical–ammonium ion system. The reaction may follow the stepwise and concerted pathways shown in Scheme 2. A first argument in favor of the prevalence of the concerted pathway results from the simulations shown in Fig. 1a of the cyclic voltammetric responses corresponding to the stepwise pathways. Using values bracketing the standard potentials and equilibrium constants of each step of the stepwise pathways, taking or not into account the presence of H-bonds (blue traces in Fig. 1a), clearly show complete

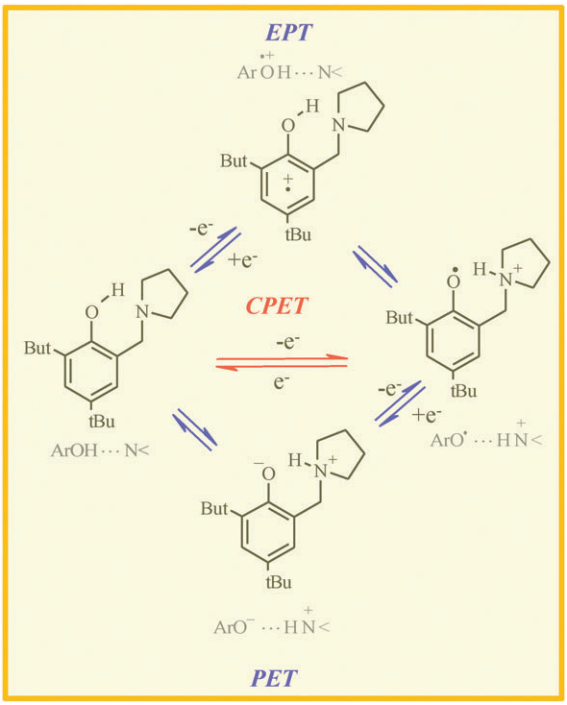

Scheme 3 PCET oxidation of a phenol bearing a proton amino group mimicking the tyrosine$_z$-histidine 190 system in Photosystem II (Scheme 1). Stepwise (blue) and concerted (red) pathways. EPT: electron transfer followed by proton transfer. PET: proton transfer followed by electron transfer. CPET: concerted proton–electron transfer.

disagreement with the low-scan rate response (red trace in Fig. 1a). An additional argument in favor of the concerted pathway is the observation of a small but significant H/D kinetic isotope effect (Fig. 1b).

What are the relationships that can be used to characterize the kinetic reactivity of the CPET pathway? Rate laws in electrochemistry relate the current i, to the red and ox reactant concentrations *at the electrode surface*, [red] and [ox], and to the driving force of the reaction. The term of "driving force" is defined as the opposite of the reaction standard free energy of the reaction, ΔG^0, with $-\Delta G^0 = F(E - E^0)$, for an oxidation reaction such as those shown in Scheme 2. E is the electrode potential and E^0, the standard potential of the redox couple. In most practical cases, this rate-driving force relationship may be linearized, thus giving rise to the so-called Butler–Volmer relationship, with a 0.5 transfer coefficient,[19] which can be expressed for an oxidation as:

$$\frac{i}{FS} = k_S^{ap} \exp\left[\frac{F}{2RT}(E - E^0)\right]\left\{[\text{red}] - \exp\left[-\frac{F}{RT}(E - E^0)\right][\text{ox}]\right\} \quad (1)$$

S is the electrode surface area, k_S^{ap}, the apparent standard rate constant, *i.e.*, the rate constant for $E = E^0$. Applicability of eqn (1) to electron transfers in the stepwise pathways is justified by the fact that they are outersphere electron transfers. Indeed, the Marcus–Hush–Levich quadratic model[16–18] may be applied in such cases and the rate law linearized over the relatively narrow potential excursion in standard cyclic

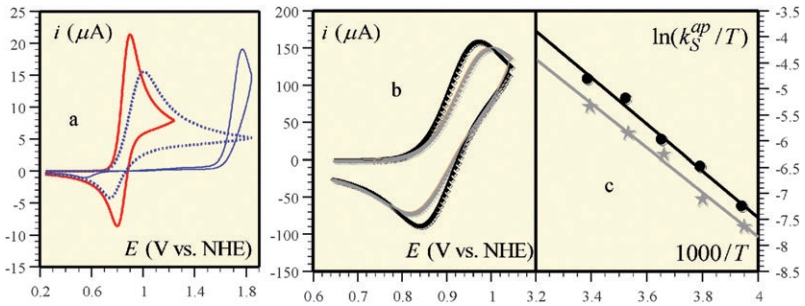

Fig. 1 Cyclic voltammetry of the aminophenol shown in Scheme 3 in acetonitrile + 0.1 M n-NBu_4BF_4. (a) in red: experimental trace at 0.2 V s^{-1}, in blue: simulation of the stepwise pathways. (b) H/D kinetic isotope effect. Cyclic voltammetry at 0.5 V s^{-1} in the presence of 2% CH_3OH (black) and CD_3OD (grey). (c) Arrhenius plots in the presence of 2% CH_3OH (black dots) and CD_3OD (grey stars).

voltammetric experiments.[19] What about the CPET reaction where not only one electron is transferred but one proton is transferred simultaneously? Justification of the applicability of eqn (1) to CPET reactions such as those represented in Scheme 3 derives from the following analysis. Assuming that proton transfer is adiabatic, the reactant state may be described by the adiabatic profile obtained, by mixing the high energy $ArO^- \cdots HN^+ <$ state with the stable $ArOH \cdots N <$ state as shown in the left downward insert of Fig. 2. Likewise, the product state may be described by the adiabatic profile obtained, by mixing the high energy $ArO^{\bullet +}H \cdots N <$ state with the stable $ArO^{\bullet} \cdots HN^+ <$ state as shown in the right downward insert of Fig. 2.

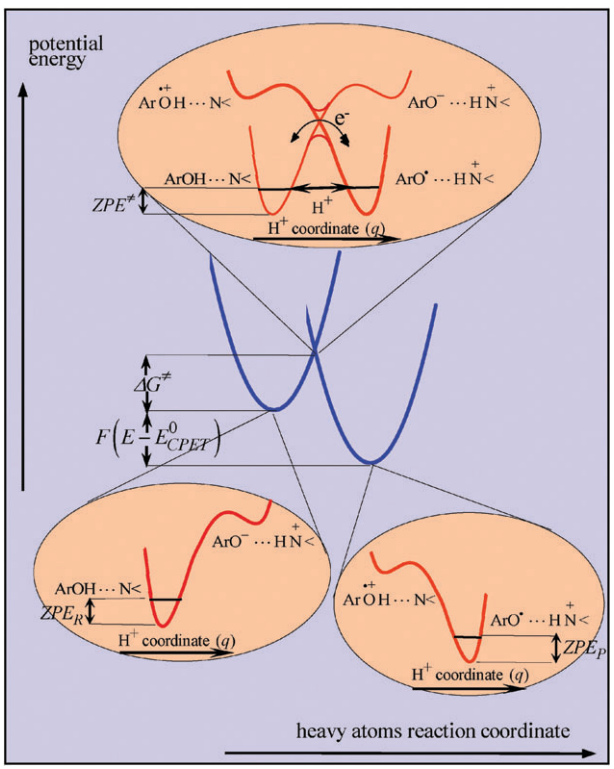

Fig. 2 CPET reactions. Potential energy profiles as a function of the heavy atom and the proton reaction coordinates in the case where the reaction only involves the proton vibrational ground states. $\Delta G^{\neq}$ is the activation free energy, ZPE_R, $ZPE^{\neq}$ and ZPE_p are the zero-point energies in the initial, transition and final states, respectively.

The Born–Oppenheimer approximation is then applied twice. Considering that both electron and proton are light particles as compared to the other atoms in the system, a first application entails that their transfer requires reorganizing solvent and heavy atoms to reach a transition state where both reactants and products have the same configuration (intersection of the blue parabolas in Fig. 2). At the transition state, the two adiabatic proton profiles deriving from the reactant and product states respectively, are mixed, under the assumption that electron transfer is adiabatic, so as to give rise to the ground-state and excited state adiabatic profiles shown in the upper insert of Fig. 2.

Since the electron is a much lighter particle than the proton, a second application of the Born–Oppenheimer approximation shows that the electron is transferred at the avoided crossing intersection of the potential energy profiles in the upper insert of Fig. 2, while the proton tunnels through the barrier thus formed. This representation applies in the case of a proton transfer occurring between two proton vibrational ground states, which is indeed often the most important contribution to the electrochemical rate constant as compared to transfers involving proton vibrational excited states.[22] In the general rate law relating the current density to the electrode potential:

$$\frac{i}{FS} = k(E)\left\{[\text{red}] - \exp\left[-\frac{F}{RT}\left(E - E^0\right)\right][\text{ox}]\right\}$$

$k(E)$, the potential-dependent rate constant may be obtained as the product of a pre-exponential factor, Z^{het}, by the classical quadratic Marcus–Hush term deriving from the harmonic approximation represented by the two crossing parabolas in Fig. 2. After linearization over the rather limited potential range scanned in usual applications of electrochemical techniques such as cyclic voltammetry, and introduction of the appropriate zero-point energy and double layer corrections, one obtains the standard rate constant (rate constant at $E = E^0$):

$$\ln(k_S^{\text{ap}}) = \ln(Z^{\text{het}}) - \left(\frac{\lambda}{4} + \frac{F}{2}\phi_S + \Delta\text{ZPE}^{\neq} - \frac{\Delta\text{ZPE}}{2}\right)\frac{1}{RT} \quad (2)$$

λ is the heavy atom-reorganization energy. $\Delta ZPE^{\neq} = ZPE^{\neq} - ZPE_R$, $\Delta ZPE = ZPE_P - ZPE_R$ are the differences in zero-point energies defined in Fig. 2. ϕ_S is the potential difference between

the reaction site and the solution, the corresponding term in equation representing the double layer effect on the kinetics.[19]

The analysis of the pre-exponential factor is based on the Landau–Zener relationship:

$$p = 1 - \exp\left[-\pi\left(\frac{C}{RT}\right)^2\sqrt{\frac{\pi RT}{\lambda}}\right]$$

in which p is the transfer probability and C represents the coupling between the reactant and product proton vibrational states at the transition state, obtained semi-classically from the ground state profile in the upper insert of Fig. 2, which we note $V(q,Q)$:

$$C(Q) = h\nu_0^{\neq}\exp\left[-2\pi/h\left(\int_{q_i}^{q_f}\sqrt{2m_P(V(q,Q)-E)}dq\right)\right]$$

where Q is the distance between the donor and acceptor atoms, q, the proton coordinate , $\nu_0^{\neq}$, the proton well frequency, m_P, the proton mass, q_i and q_f the classical turning points in each well at fixed Q. It follows that p is a function of Q to be averaged over the Boltzmann distribution, thus emphasizing the importance of small values of Q in proton tunneling.

A first description of the CPET electrochemical kinetics was based on the assumption that the electron transfer, concerted with proton transfer, occurs when the reactant is at a given distance from the electrode, referred to as the reaction site, usually assumed to be located at the outer Helmholtz plane.[26] Applying the preceding equations to all electronic states of the electron in the electrode led, after linearization, to eqn (1) and (2) and to the following expression of the pre-exponential factor:

$$Z^{het} = \chi k_{coll}^{het}\sqrt{\frac{RT}{4\pi\lambda^{het}}}\frac{1}{\sqrt{1+\pi RT/\lambda^{het}}} \simeq \chi k_{coll}^{het}\sqrt{\frac{RT}{4\pi\ \lambda^{het}}}$$

k_{coll}^{het} is the heterogeneous collision frequency. $\chi = 2p/(1 + p)$, the transmission coefficient is a measure of proton tunneling through the transition state barrier (see upper insert in Fig. 2) and therefore of the degree of adiabaticity.

The H/D kinetic isotope effect is reflected in two ways in the model. One derives from the zero-point energy terms in the slope of the Arrhenius plot (see eqn (2)). The other is contained in the pre-exponential factor and reflects proton tunneling through the transition state barrier, if any. If the CPET reaction is adiabatic, the H/D kinetic isotope effect only appears in the zero-point energy terms in the Arrhenius slope. In the treatment of ref. 26, based on the collision frequency, the H/D kinetic isotope effect on the pre-exponential factor was neglected, considering that the reaction was adiabatic, retaining only the zero-point energy effect.

A more elaborate recent analysis[27] takes into account the fact that the reaction may take place at various distances from the electrode surface, similarly to what happens with simple outer-sphere electron transfer reactions,[27,28] leading to the conclusion that the electrochemical reaction is non-adiabatic. From the distance between the two Arrhenius plots in Fig. 1c, the H/D kinetic isotopic effect may be estimated as being equal to 3.5, a value that falls in line with the CPET reaction being non-adiabatic. Derived from the Arrhenius slope, the reorganization energy was estimated to be 1.5 eV.

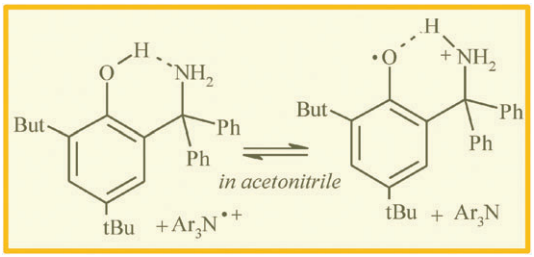

Scheme 4 Homogeneous PCET oxidation of a phenol bearing a proton amino group mimicking the tyrosine$_z$–histidine 190 system in Photosystem II (Scheme 1) by a series of triarylamine cation radicals.[29,30]

It is interesting to compare the above results to those obtained in the oxidation of a similar amino phenol (Scheme 4) by a series of triarylamine cation radicals used as homogeneous reactants.[29,30] In this case too, the slope of linearized Arrhenius plot led, taking due account of the variations of the thermodynamics of the reaction with temperature, to an estimation of the reorganization energy.[22,27] The value thus found, 1.1 eV for the self-exchange reaction of the aminophenol of Scheme 4, is compatible within experimental uncertainty with the electrochemical value found for the slightly different aminophenol of Scheme 3. Analysis of the intercept of the Arrhenius plot taking into account that the reaction may take place at various inter-reactant distances,[31] pointed to a non-adiabatic reaction.[27]

2.2 Phenols with attached carboxylate groups as proton acceptor

Aside amines, other basic groups attached to the phenol structure are susceptible to be efficient proton acceptors. This is the case with carboxylate groups, also frequent in natural systems, which indeed play a similar role as illustrated by the example depicted in Scheme 5 where the *ortho*,*ortho*′-dicarboxylatohydrobenzoquinone is electrochemically oxidized to the semiquinone with concerted transfer of the proton to the carboxylate.[32] A CPET pathway is also taken for the further oxidation, generating benzoquinone with proton transfer to the second carboxylate, finally yielding the quinone dicarboxylic acid.

3. Phenol oxidation in water with water as the proton acceptor

Water is the solvent in innumerable natural and industrial systems and may at the same time play the role of proton donor and acceptor in PCET reactions. It is however a peculiar, H-bonded and H-bonding proton donor and acceptor. These peculiar properties manifest themselves in the mechanisms of proton conduction, which remain under active experimental and theoretical scrutiny in spite of having been investigated over decades.[33,34] How these peculiar characteristics influence the mechanism of PCET reactions involving water should deserve the same attention.

PCET oxidation of phenols in water (Scheme 6) usually yields dimers resulting from coupling of the phenoxyl radicals produced upon electron and proton transfer, thus adding a

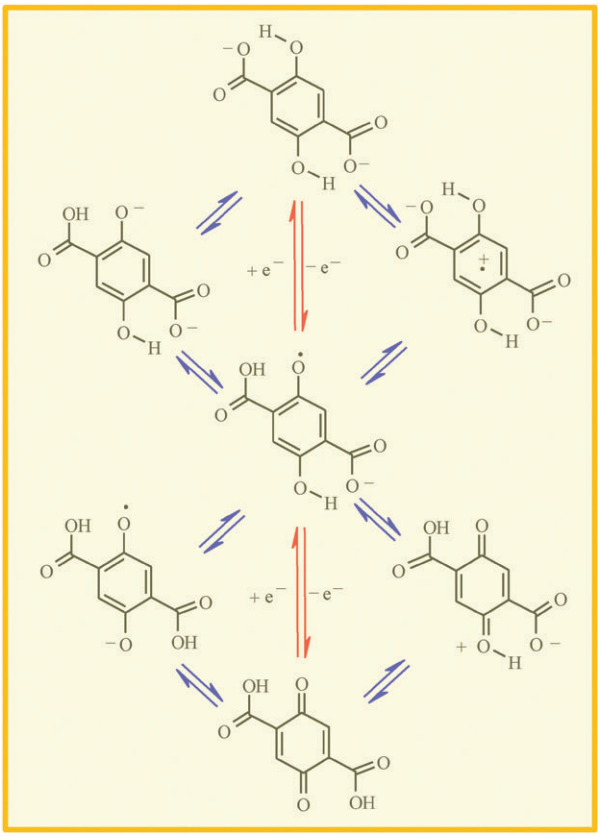

Scheme 5 Two-electron electrochemical oxidation of *ortho*,*ortho*′-dicarboxylatohydrobenzoquinone.[32] Red arrows: CPET pathways. Blue arrows: stepwise pathways.

complicating feature to the investigation of the PCET mechanism. A way of obviating this difficulty consists in protecting the phenoxyl radical against dimerization by the presence of *tert*-butyl groups in *ortho*, *ortho*′ and *para* positions (Fig. 3a).[35] The variation with pH of the apparent standard potential, E^0_{ap}, defined from the Nernst law:

$$E = E^0_{ap} + \frac{RT}{F}\ln\left(\frac{[ArO^{\bullet}] + [ArOH^{\bullet+}]}{[ArOH] + [ArO^{-}]}\right) \qquad (3)$$

shown in Fig. 3b (Pourbaix plot), indicates that the only thermodynamically stable species within the range of accessible pHs are the starting phenol and the final phenoxyl radical. The variations of the cyclic voltammetric traces in non-buffered 50/50 water–ethanol with pH (Fig. 3c)[36] indicate that a PET pathway is followed at high pHs, the first reversible wave standing for the oxidation of the phenoxide ion into the phenoxyl radical, which is further oxidized at the second wave. Lowering the pH results in a decrease of the first wave, which ultimately vanishes at the benefit of an intermediate wave. The latter corresponds to the CPET pathway as confirmed by a significant H/D effect. Cyclic voltammetry thus allows an easy visualization of the competition between the PET and CPET pathways that is represented by two successive reversible waves of comparable height at pH = 10.5 (Fig. 3d). The appearance of the two waves was made possible by the use of a non-buffered medium in which the diffusion of OH^- and H^+

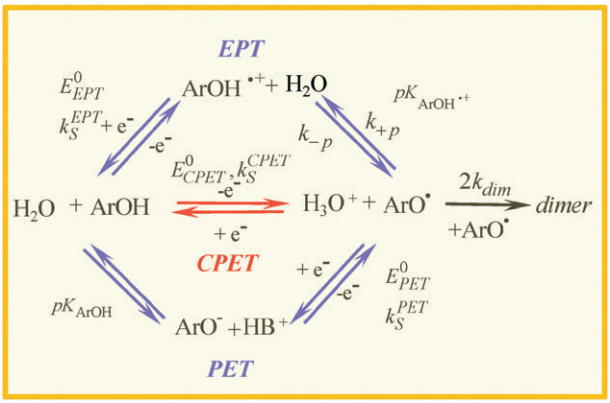

Scheme 6 Stepwise and concerted pathways for the oxidation of phenols. Ar: phenyl or other aryl groups, $ArOH^{\cdot+}$: cation radical of ArOH.

participate in rate determination as confirmed by the simulation shown in Fig. 3d.

In spite of the drawbacks deriving from dimerization, the electrochemical oxidation of simple phenol may be successfully analyzed provided two conditions are fulfilled. One is that the phenol concentration be low enough and the cyclic voltammetry scan rate high enough for self inhibition by the dimer precipitating onto the electrode surface be negligible (tests are easily performed with the straightforward oxidation of phenoxide ion as can be observed in basic medium).

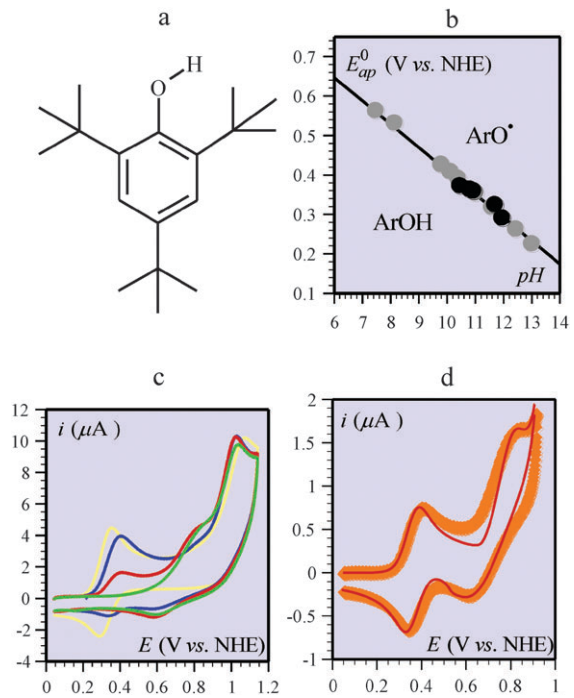

Fig. 3 CPET reactions. (a) 2,4,6-tri-*tert*-butyl phenol. (b) apparent standard potential *vs.* pH in 50/50 water–ethanol, in Britton–Robinson buffers (grey dots) and non-buffered (black dots) solutions. (c) cyclic voltammetry of 0.28 mM 2,4,6-tri-*tert*-butyl phenol in non-buffered 50/50 water–ethanol at 0.1 V s^{-1}, pH = 8.2 (green), 10.5 (red), 11 (blue), 11.7 (yellow). (d) thick orange line: same conditions as in (c) for pH = 10.5 with the potential scanning limited to the first two waves. Thin red line: simulation.

The second condition is that the rate of dimerization, obtained from pulse radiolysis experiments be inserted in the kinetic analysis.

The thermodynamics of the reaction were derived from the cyclic voltammograms obtained in buffered media (Fig. 4), taking into account the dimerization rate constant.[37] The peak potentials, E_p of all voltammograms obtained as a function of pH (Fig. 4a) obey eqn (4):

$$E_p = E^0_{ap} + 0.903RT/F - (RT\ln 10/3F)\log(4RTk_{dim}C^0/3Fv) \quad (4)$$

in which E^0_{ap} is the pH-dependent apparent standard potential defined in eqn (3). v and C^0 are the scan rate and phenol concentration respectively. This fast $e^- + H^+$ exchange, obeying the Nernst law, is followed by a rate determining dimerization, with a rate constant, k_{dim}, thus giving rise to eqn (4) (chapter 2 in ref. 19). The thickness of the wave (difference between peak and half-peak potentials) is also indicative of this reaction sequence. Application of eqn (4) with $2k_{dim} = 2.6 \times 10^9$ M^{-1} s^{-1} as derived from pulse radiolysis,[38] leads to the Pourbaix diagram in Fig. 4c, which defines the zones of thermodynamic stability of the various intervening species and the values of all characteristic pKs and standard potentials ($pK_{ArOH^{\bullet+}} = -2$ is obtained from an independent source).[39] In gauging the driving force of the CPET reaction from the difference between its characteristic standard potential and the electrode potential, it should be borne in mind that the nature of the proton acceptor has to be precisely defined. For example, if water is the proton acceptor, the CPET standard potential is equal to the apparent standard potential at pH = 0 (Fig. 4c). If the proton acceptor were to be the diphosphate ion, the CPET standard potential would be equal to the apparent standard potential at $pH = pK_{PO_4H_2^-} = 7.2$. In no case does the actual standard potential, and henceforth the driving force, vary with pH,[40,41] as sometimes incorrectly stated.[42–45]

For reasons that will be detailed later on, PCET kinetics and mechanisms are more accessible from experiments carried out in unbuffered media such as those summarized in Fig. 5. The cyclic voltammetric responses obtained in unbuffered media (Fig. 5a) are drastically different from those obtained in buffered media (Fig. 4a). Starting from the most basic media where a single wave appears on the less positive side of the potential range, the wave splits into two waves upon decreasing pH. The first wave, which takes place in the same potential region as in buffers, rapidly decreases with pH at the expense of a more positive second wave. When the latter wave is fully developed, the variations of its peak potential with pH (Fig. 5b) also strongly differ from those observed in buffered media (Fig. 4b). The first wave thus appears to correspond to the oxidation of phenoxide ion as in the same buffered pH region. The only base in the unbuffered medium that is able to deprotonate phenol is OH^-. Above the phenol pK, the phenoxide ion predominates and the reaction simply continues in its oxidation, yielding the phenoxyl radical, which eventually dimerizes. As the pH decreases below this pK, fast deprotonation of phenol by the OH^- ions present continues to produce the phenoxide ion and hence the radical and the dimer

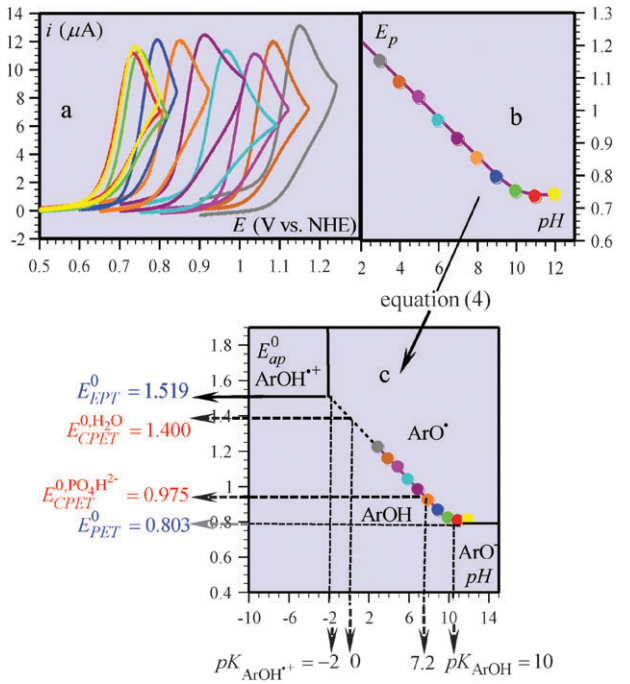

Fig. 4 Cyclic voltammetry of 0.2 mM phenol in 0.1 M Britton–Robinson buffers at 0.2 V s^{-1} (a) at pH s that are reported in (b) where the peak potential are plotted against pH using the same color code as in (a). (c) Pourbaix diagram obtained from the application of eqn (4) to the data in (b).

along an OH^--triggered PET pathway. Under the unbuffered conditions, two factors govern the kinetics of the PET pathway. One of these, taking into account that deprotonation of phenol is very fast, is diffusion of OH^- ions toward the electrode. Phenol concentration is another essential parameter since it determines the amount of proton equivalents that are generated upon oxidation, making the pH decrease during the course of the cyclic voltammetric experiment. These factors can be put together within a kinetic model that leads to an integral equation describing the current–potential response.[37] Application of this equation, using the parameter values listed in Table 1, leads to a satisfactory reproduction of the experimental data (Fig. 5c).

As the first wave vanishes upon decreasing the pH, the PET pathway shuts down and the question arises of the mechanism, EPT or CPET, of the reaction taking place at the henceforth predominating second wave. Once the first wave has completely disappeared, the location of the second wave remains the same down to pH = 4, with a peak potential (Fig. 5b) well above its value in buffered media. It then catches up with the buffered medium-59 mV-slope straight line. Such a behavior derives from the absence of buffering and the according decrease of pH during the course of the cyclic voltammetric experiment, whenever the reaction follows the EPT or CPET pathway. Diffusion of the protons produced in both cases at the electrode thus becomes an essential rate-controlling factor. Phenol concentration is accordingly an important parameter since it determines the maximal amount of protons produced. Upon decreasing the pH, the total amount of protons produced becomes small as compared to the concentration of protons

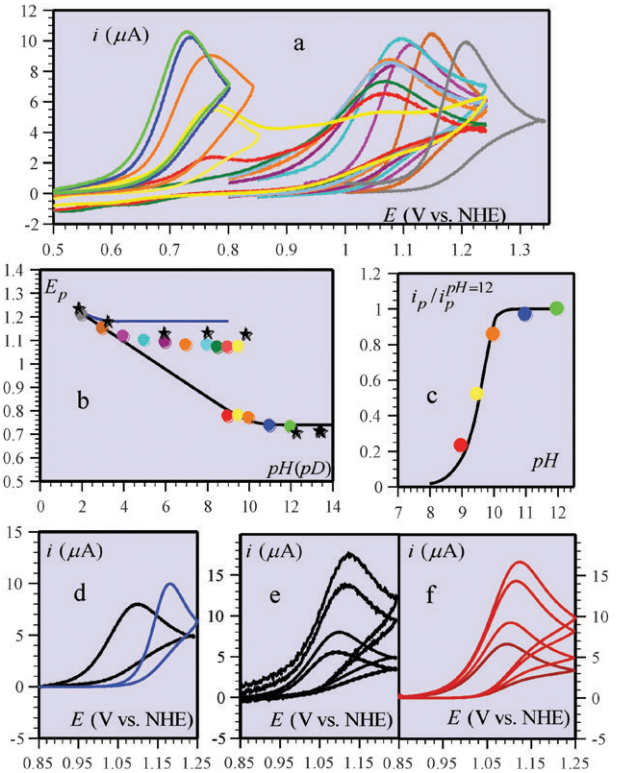

Fig. 5 Oxidation of phenol in unbuffered water. (a) Cyclic voltammetry of 0.2 mM PhOH in unbuffered water at 0.2 V s^{-1} as a function of pH: from right to left: 2, 3, 4, 5, 6, 7, 8, 8.5, 9, 9.5, 9.5, 10, 11, 12. (b) dots (with the same color code as in (a)) peak potential as a function of pH. Black line: variation of the peak potential in 0.05 M Britton–Robinson buffers. Black stars: unbuffered heavy water, blue line simulation according to a Nernstian EPT mechanism. (c) basic unbuffered water (first five voltammograms of Fig. 5a, with the same color code) showing the decrease of the peak current with the pH (dots) compared to the simulation (full line, see text and the parameter values in Table 1) of an OH^--PET pathway. The peak currents, i_p, are normalized toward the value at pH = 12. (d) black: cyclic voltammogram at pH = 7.2 and 0.2 V s^{-1}; blue: simulation for an EPT mechanism. (e) cyclic voltammetry at pH = 7.2 as a function of scan rate: from bottom to top: 0.1, 0.2, 0.5, 0.7 V s^{-1}. (f) simulation of the voltammograms in (e) for a CPET mechanism.

already present, leading to the same behavior as observed in the buffered media of same pH in term of peak potentials (Fig. 5b).

The further step in the mechanism analysis is to discriminate between the EPT and CPET pathway. The EPT mechanism can be ruled out according to an *a fortiori* argument: the best conditions for this mechanism is an infinitely fast electron transfer step, giving rise to a Nernstian behavior, followed by a maximally fast proton transfer (10^{13} s^{-1}, corresponding to 10^{11} M^{-1} s^{-1}, for the reprotonation step, since $pK_{ArOH^{\bullet+}} = -2$). The peak potentials thus predicted are much too positive compared to the experimental peak potentials (Fig. 5b and d). The voltammogram shapes do not agree as well as seen in Fig. 5d.

Having thus unambiguously established the occurrence of the CPET mechanism, we note the CPET peak potentials shift in the positive direction from H_2O to D_2O (Fig. 5b), indicating the interference of the CPET kinetics besides proton diffusion. Additional experiments were consequently carried out as a function of the scan rate at pH 7.2, in the middle of the pH range of interest, in view of characterizing the kinetics of the CPET reaction (Fig. 5e). A model was developed to simulate the cyclic voltammetric responses expected with such a mechanism. It is based on the approximation of CPET kinetic by a Butler–Volmer law with a transfer coefficient of 0.5:

$$\frac{i}{FS} = k_S^{CPET} \exp\left[\frac{F}{2RT}\left(E - E^0_{CPET}\right)\right] \times \left\{[ArOH]_0 - \frac{[ArO^{\bullet}]_0[H^+]_0}{C_S}\exp\left[-\frac{F}{RT}\left(E - E^0_{CPET}\right)\right]\right\}$$

(the $[\,]_0$ are the concentrations at the electrode surface in mol L^{-1} and C_S is the standard concentration taken as equal to 1 mol L^{-1}) in which the back reaction term has been modified to take into account its ternary character (one electrode and two molecules) whereas the forward term has the usual form because, water being the solvent, its concentration and activity are constant. Because the reaction medium is not buffered, diffusion of protons is an important rate-controlling factor, besides electron transfer and phenoxyl dimerization, as illustrated by the expression of the competition parameter:

$$p_{unbuffered} = \frac{k_S^{CPET}(C^0/C_S)^{1/2}}{(D_{ArOH})^{1/4}(D_{H^+})^{1/4}(Fv/RT)^{1/3}(4k_{dim}C^0)^{1/6}}$$

(C^0: phenol bulk concentration, v: scan rate, Ds diffusion coefficients of the subscript species).

Simulation (Fig. 5f) of the experimental voltammograms (Fig. 5e) led to $k_S^{CPET} = 25 \pm 5$ cm s^{-1}.

The reason that such a high value of an electrochemical standard rate constant could be reached at very moderate scan rates is not only that the follow-up dimerization tends to make the preceding electron transfer the rate-determining step in unbuffered as in buffered media but that this tendency is stronger in unbuffered media because reprotonation of $ArO^{\bullet}$

Table 1 Simulation parameters

Potentials/V *vs.* NHE: $E^{dim}_{PET} = 0.714$, $E^0_{PET} = 0.803$
$E^0_{EPT} = 1.519$, E^0_{CPET} (H_2O) 1.400, E^0_{CPET} (D_2O) = 1.421
Diffusion coefficients $\times 10^5$/cm^2 s^{-1}: $D_{PhOH} = 3.7$, $D_{OH^-} = 5.4$, $D_{H^+} = 9.3$, $D_{D^+} = 6.6$,[46] $D_{PO_4H^{2-}} = 1$
Standard rate constants/cm s^{-1}: k_S^{CPET} (H) = 25 ± 5, k_S^{CPET} (D) = 10 ± 2
Rate constants/M^{-1} s^{-1}: $2k_{dim} = 2.6 \times 10^9$

is more difficult as attested by the terms C^0/C_S and D_{H^+} in $p_{unbuffered}$, which are absent in the expression the competition parameter would have in buffered media: [47]

$$p_{buffered} = \frac{k_S^{CPET}}{(D_{ArOH})^{1/2}(Fv/RT)^{1/3}(4k_{dim}C^0/3)^{1/6}}$$

$p_{unbuffered}$ = 0.5 at 0.2 V s^{-1} indicating a mixed kinetic control by electron transfer and dimerization, which allows the determination of the standard rate constant. In a buffer medium at pH = 0 and same scan rate, $p_{buffered}$ = 200, leaving no chance for electron transfer to participate in the kinetic control within the accessible range of scan rates. Repeating the same experiments and analyses in heavy water led to: k_S^{CPET} (D) = 10 ± 2 cm s^{-1}, *i.e.*, a H/D kinetic isotopic effect of 2.5. The occurrence of the CPET mechanism is thus confirmed and the value of the H/D kinetic isotopic effect falls in line with a quasi-adiabatic reaction.

It is interesting to examine whether such a fast standard rate constant is also found in the oxidation of phenol by homogeneous electron acceptors (the concept of standard rate constant is less frequently used in homogeneous electron transfer chemistry than in electrochemistry, although it can be defined in the same manner as the rate constant at zero driving force). In this connection, laser flash photolysis, redox catalysis and stopped-flow have been recently used to investigate the variation of the oxidation rate constant of phenol in neat water with the driving force offered by a series of electron acceptors, ruthenium(III) trisbipyridine and substituted analogs.[48] Taking into account results previously obtained with a low-driving force electron acceptor, $IrCl_6^{2-}$,[49] thus allowed scanning more than half an electron-volt driving force range. Variation of the overall rate constant, k_+, with pH showed the transition between a direct phenol oxidation reaction at low pH, where the rate constant, k_1, does not vary with pH and a stepwise reaction involving the prior deprotonation of phenol by OH^-, followed by the oxidation of phenoxide ions with a rate constant k_2:

$$k_+ = \frac{[ArOH]}{[ArOH]_{total}}k_1 + \frac{[ArO^-]}{[ArOH]_{total}}k_2 \qquad (5)$$

The transition between phenol and phenoxide ion oxidation is characterized by a unity-slope variation (Fig. 6). In no case did these data show the 1/2 slope previously reported for the oxidation of phenol by $Ru^{III}(bpy)_3$.[44] The latter behavior was explained by means of the incorrect notion of pH-dependent driving force as discussed previously.

Analyses of the oxidation kinetics, based on its variation with the driving force, *i.e.*, the opposite of the standard free enthalpy of reaction $-\Delta G^0_{CPET} = F(E^0_{acceptor} - E^0_{CPET})$ shown in Fig. 6d (the data point for the Ru^{III}(4,4′-methyl-bpy)$_3$ complex was determined at a single pH, 3, for the electron acceptor, Ce^{IV} is not stable at higher pHs).

Based on these data and on the determination of H/D isotope effects, a stepwise mechanism in which electron transfer is followed by the deprotonation of the initial cation radical could be ruled out at the benefit of a CPET pathway. Derivation of the characteristics of counter-diffusion in termolecular reactions allowed showing that the concerted process is under activation control. It is characterized by a remarkably large standard rate constant, 10^7 $M^{-1}s^{-1}$ (Fig. 6d) which falls in line with the electrochemical data and underpins the very peculiar behavior of water as proton acceptor when it is used as the solvent. As in the electrochemical case, a small but significant H/D kinetic isotope effect is observed (Fig. 6d).

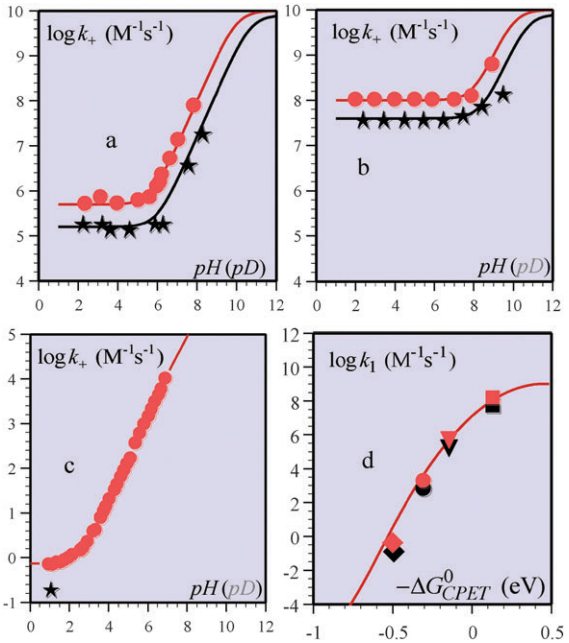

Fig. 6 Variation with pH (or pD) of the overall forward rate constant of phenol + phenoxide oxidation by the various electron acceptors. (a) $Ru^{III}(bpy)_3$, (b) Ru^{III}(4,4′- CO_2Et-bpy)$_2$(bpy). (c) $Ir^{IV}Cl_6$. Red dots: results obtained in H_2O by the laser flash technique in (a), and (b) and by the stopped-flow method in (c) (from ref. 49). Black stars: results obtained in the same way in D_2O. Red and black lines: application of eqn (5) to the H_2O and D_2O data, respectively (parameter values in Table 1). (d) forward rate constant of phenol oxidation by the various electron acceptors. Red and black symbols for H_2O and D_2O, respectively; squares: $Ru^{III}(bpy)$.

4. Inserting an hydroxylic H-bond relay between proton exchanging sites

The preceding section has emphasized the rapidity of concerted proton electron transfer when water, used as solvent, plays simultaneously the role of proton acceptor. The exact causes of this rapidity are not known for the moment but they are likely to be related to the H-bonded and H-bonding properties of the water molecules. These properties have already been shown to be the origin[50] of the considerable acceleration of the electrochemical reduction of superoxide ions in an aprotic medium triggered by addition of water.[51–52] Whether water chains are involved in long-distance CPET reactions, as they are in long-distance proton transfer and transport,[33,34,53] is an issue of timely interest.

In biomimetic molecules such as those discussed in Section 2, the distance over which the proton may travel as the result of a CPET reaction is limited to values compatible with the

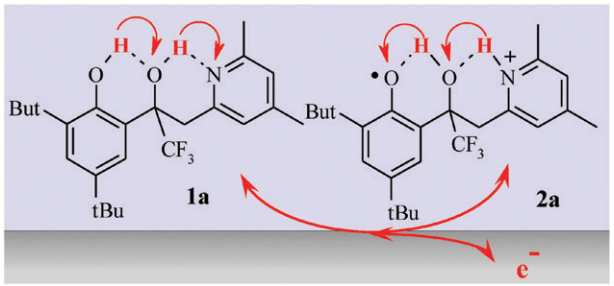

Scheme 7 An example of CPET reaction where proton transfer is relayed by an H-bond donating and accepting hydroxylic group.

formation of an H-bond in the starting molecule. The idea according to which this distance might be substantially increased by inserting a hydrogen-bond relay between the group being oxidized and the distant proton acceptor has been recently explored.[54] In this purpose the oxidation of the molecule shown in Scheme 7 was investigated by means of cyclic voltammetry. The proton relay in this molecule is an OH group. It is able to accept an H-bond from the phenol being oxidized and, at the same time, to form an H-bond with the amine proton accepting group, without going through a protonated state in the course of the reaction. The CF_3 group was introduced to reach a good balance between these two properties.

The choice of an electrochemical approach rather than an homogeneous oxidation approach, for testing the occurrence of the CPET reaction depicted in Scheme 7, was mainly dictated by the fact that an electrochemical non-destructive technique such as cyclic voltammetry allows a quick investigation of a continuous range of driving forces, leading to the determination of a standard rate constant (rate constant at zero driving force). The main features of the typical cyclic voltammogram shown in Fig. 7-**1a** are a one-electron stoichiometry and a chemical reversibility indicating that the cation radical **2a** (Scheme 7) is stable within the time-scale of slow scan cyclic voltammetry. **2a** is actually stable over much longer times as results from its formation upon a preparative-scale electrolysis beyond the cyclic voltammetric peak, which is characterized by a typical phenoxyl radical UV-vis spectrum and the infrared signature of protonation of the pyridine group.

The reversibility and one-electron stoichiometry of the cyclic voltammetric response in Fig. 7-**1a** contrasts with the irreversibility and two-electron stoichiometry observed when neither the pyridine acceptor, nor the OH relay are present as with 2,4,6-tri-tertbutyl phenol (Fig. 7-**1c**). In the latter case,[35] the cation radical initially formed rapidly and irreversibly deprotonates yielding the phenoxyl radical that is oxidized more easily than the starting phenol according to a two-electron stoichiometry "ECE" mechanism (chapter 2 in ref. 19). The same behavior is also observed in the presence of the OH relay and in the absence of the pyridine moiety (Fig. 7-**1d**). It follows that the reversible oxidation of **1a** does not go through the cation radical bearing a positive charge on the central OH group. That the reaction does not go through an intermediate in which the central alcohol would be protonated is further substantiated by the pK values in acetonitrile of phenol, 27, and protonated alcohol, <2.

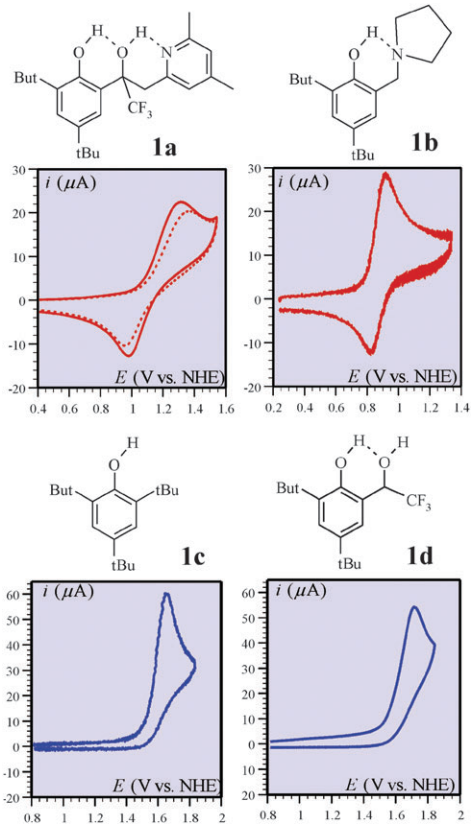

Fig. 7 Cyclic voltammetry in acetonitrile + 0.1 M $nNBu_4BF_4$ of 1 mM of the compounds shown on top of each diagram at a glassy carbon electrode and a scan rate of 0.2 V s^{-1}. In **1a**, the solid and dashed traces were recorded in the presence of 1% CH_3OH and CD_3OD, respectively.

The cyclic voltammogram in Fig. 7-**1a** resembles more that of the aminophenol **1b** in Fig. 7-**1b** in terms of both electron stoichiometry and chemical reversibility, although the anodic-to-cathodic potential separation is larger in the first case than in the second. As shown in Section 2, the proton generated upon one-electron oxidation of the phenol moiety is transferred to the amine group concertedly with electron transfer thanks to a six-member ring configuration favorable to the formation of an H-bond between the phenol and amine group in the starting molecule. With **1a**, proof that the alcoholic OH group effectively serves as a H-bond relay between the phenol and pyridine groups, requires that the molecule is not folded so as to put these two groups at a sufficiently short distance one from the other to bring about the direct formation of an H-bond between them. The X-ray structure of **1a** indeed shows that this is the case, the distance between the phenolic oxygen and the pyridine nitrogen is indeed 4.44 Å and the $O_2O_1C_1N_1$ dihedral angle is equal to 113.9°.[54] DFT calculations led to practically the same result in the case of **1a** and showed additionally that the cation radical, **2a**, is not substantially folded as well.

Additional evidence that a concerted pathway is indeed followed in the oxidation of **1a** is the observation of an H/D kinetic isotope effect (KIE), very similar to what was previously observed with **1b**. In other words, the reaction sketched in Scheme 7 is not merely the expression of a global process but

should be viewed as an elementary CPET step. This conclusion also falls in line with the unlikeness of a mechanism that would go through oxidation of the zwitterionic form of **1a**:

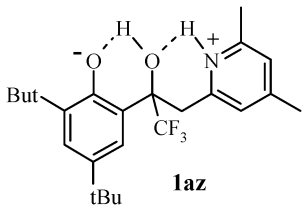

1az

owing to the smallness of the equilibrium ratio:

$$\frac{[\mathbf{1az}]}{[\mathbf{1a}]} \simeq 10^{-\left(pK_{PhOH} - \frac{pK_{2,4,6\text{-trimethylpyridine}} + pK_{2,4\text{-dimethylpyridine}}}{2}\right)} \simeq 10^{-9}$$

The anodic-to-cathodic peak separation is larger with **1a** than with **1b** denoting a slower CPET reaction ($k_S = 5 \times 10^{-4}$ cm s^{-1}) in the first case than in the second ($k_S = 8 \times 10^{-3}$ cm s^{-1}), presumably related to a more important intramolecular reorganization.

It may thus be concluded that the introduction of an H-bonding group between the electron and proton exchanging sites may offer an efficient route for proton movement over distances as large as 4.3 Å, by means of translocation of two protons concerted with electron transfer. This Grotthuss proton transfer is as efficient as the travel it accomplishes over distances of the order of 2.5 Å in systems where H-bonding between the phenol and the proton acceptor benefits from the formation of a six-member ring. The key feature of this efficient proton transport is the H-bond swing represented in Scheme 7, which avoids a high-energy protonated relay intermediate.

5. Conclusions

The oxidation of phenols is an extremely important reaction in many areas of natural and artificial chemistry, where electron transfer is inevitably associated with proton transfer. Among mechanism analyses that have attempted to decipher the competition between stepwise and concerted pathways, the electrochemical and homogeneous oxidation of phenols is undoubtedly the best example of successful characterization of concerted pathways (CPET reactions). This has been the case with amino-phenols mimicking the tyrosine–histidine couple in Photosystem II. The theoretical model developed on this occasion, based on a successive double application of the Born–Oppenheimer approximation, leads to a current–potential relationship that can be linearized under most practical circumstances and is characterized by two main parameters. One deals with the reorganization of all heavy atoms involved in the reactants and in the solvent. The other, which appears in the pre-exponential factor of the rate law, is related to proton tunneling and to the existence of an H/D kinetic isotope effect, the magnitude of which increases with the non-adiabatic character of the reaction. The model applies both to electrochemical oxidation and oxidation by homogeneous reagents.

The advantage of the electrochemical approach, through techniques like cyclic voltammetry, is twofold. On the one hand, the driving force may be continuously varied by means of the electrode potential; on the other the current is an easy measure of the reaction kinetics even if diffusion of reactants has to be taken into account in the kinetic analysis.

Oxidation of phenols when water is both the solvent and the proton acceptor is another example where the concerted pathway has been shown to prevail over the stepwise pathways, except in basic media where the reaction involves the oxidation of the phenoxide ion resulting from the deprotonation of the phenol by OH^-. The reaction is characterized by an extremely high standard rate constant (rate constant at zero driving force) both in electrochemistry and in homogeneous oxidations. Although the exact reasons that these reactions are so intrinsically fast are not fully elucidated at present, there are presumably related to the H-bond donating and H-bond accepting character of the water molecules and to their resulting association.

The H-bond donating and H-bond accepting properties of a molecular center was further exploited to create an H-bond relay between in the transport of protons triggered concertedly by electron transfer over large distances. The conditions of an appropriate balance between the H-bond donating and H-bond accepting properties were found empirically but would deserve systematization in the future. Other molecular models involving promoting long-distance proton transport triggered by electron transfer associating water molecules and protein-like environments would be also worth investigating.

Contemporary energy issues involve catalytic oxidation and reduction of simple molecules like dioxygen, protons, water carbon dioxide in which coupling between proton and electron transfer is likely to be crucial. In this connection, reactions in which electron transfer is concerted not only with proton transfer but also with the cleavage of bonds between heavy atoms (for example O–O bond) will certainly be worth investigating at the experimental and theoretical level in the next future.

Acknowledgements

Julien Bonin, Cyril Louault, Mathilde Routier and Cédric Tard are thanked for their participation to the work described in this article. Partial financial support from the ANR PROTOCOLE is gratefully acknowledged.

Notes and references

1 C. Tommos and G. T. Babcock, *Biochim. Biophys. Acta, Bioenerg.*, 2000, **1458**, 199.
2 G. Renger, *Biochim. Biophys. Acta, Bioenerg.*, 2004, **1655**, 195.
3 T. J. Meyer, M. H. V. Huynh and H. H. Thorp, *Angew. Chem., Int. Ed.*, 2007, **46**, 5284.
4 A. W. Rutherford and A. Boussac, *Science*, 2004, **303**, 1782.
5 J. Stubbe, D. G. Nocera, C. S. Yee and M. C. Y. Chang, *Chem. Rev.*, 2003, **103**, 2167.
6 L. L. Williams, *J. Am. Chem. Soc.*, 2004, **126**, 12441.
7 N. Cotelle, P. Hapiot, J. Pinson, C. Rolando and H. Vezin, *J. Phys. Chem. B*, 2005, **109**, 23720.
8 R. D. Webster, *Acc. Chem. Res.*, 2007, **40**, 251.
9 J. Ralph, K. Lundquist, G. Brunow, F. Lu, H. Kim, P. F. Schatz, J. M. Marita, R. D. Hatfield, S. A. Ralph, J. H. Christensen and W. Boerjan, *Phytochem. Rev.*, 2004, **3**, 29.
10 R. Vanholme, K. Morreel, J. Ralph and W. Boerjan, *Curr. Opin. Plant Biol.*, 2008, **11**, 278.

11 G. W. Morrow, in *Anodic Oxidation of Oxygen-Containing Compounds*, ed. H. Lund and O. Hammerich, Organic Electrochemistry, Marcel Dekker, New York, 4th edn, 2001, pp. 589–620.
12 L. Biczok and H. Linschitz, *J. Phys. Chem.*, 1995, **99**, 1843.
13 B. Kok, B. Forbush and M. McGloin, *Photochem. Photobiol.*, 1970, **11**, 457.
14 K. N. Ferreira, T. M. Iverson, K. Maghlaoui, J. Barber and S. Iwata, *Science*, 2004, **303**, 1831.
15 B. Loll, J. Kern, W. Saenger, A. Zouni and J. Biesiadka, *Nature*, 2005, **438**, 1040.
16 R. A. Marcus, *Electrochim. Acta*, 1958, **13**, 955.
17 N. S. Hush, *Electrochim. Acta*, 1968, **13**, 1005.
18 V. G. Levich, *Present State of the Theory of Oxidation-Reduction in Solution (Bulk and Electrode Reactions)* in Advances in Electrochemistry and Electrochemical Engineering, ed. P. Delahay and C. W. Tobias, Wiley, New York, 1955, pp. 250–371.
19 J.-M. Savéant, *Elements of Molecular and Biomolecular Electrochemistry*, Wiley-Interscience, New York, 2006.
20 E. Laviron, *J. Electroanal. Chem.*, 1981, **124**, 1.
21 C. Costentin, M. Robert and J.-M. Savéant, *J. Electroanal. Chem.*, 2006, **588**, 197.
22 C. Costentin, M. Robert and J. M. Savéant, *J. Am. Chem. Soc.*, 2007, **129**, 9953; C. Costentin, M. Robert and J.-M. Savéant, *J. Am. Chem. Soc.*, 2010, **132**, 2845 (correction).
23 S. Hammes-Schiffer, *Acc. Chem. Res.*, 2009, **42**, 1881.
24 P. M. Kiefer and J. T. Hynes, *J. Phys. Chem. A*, 2004, **108**, 11793.
25 T. Maki, Y. Araki, Y. Ishida, O. Onomura and Y. Matsumura, *J. Am. Chem. Soc.*, 2001, **123**, 3371.
26 C. Costentin, M. Robert and J.-M. Savéant, *J. Am. Chem. Soc.*, 2006, **128**, 4552.
27 C. Costentin, M. Robert, J.-M. Savéant and C. Tard, *Angew. Chem., Int.Ed.*, 2010, **49**, 3803.
28 S. W. Feldberg and N. Sutin, *Chem. Phys.*, 2006, **324**, 216.
29 I. J. Rhile and J. M. Mayer, *J. Am. Chem. Soc.*, 2004, **126**, 12718.
30 I. J. Rhile, T. F. Markle, H. Nagao, A. G. DiPasquale, O. P. Lam, M. A. Lockwood, K. Rotter and J. M. Mayer, *J. Am. Chem. Soc.*, 2006, **128**, 6075.
31 N. Sutin, *Acc. Chem. Res.*, 1982, **15**, 275.
32 C. Costentin, M. Robert and J. M. Savéant, *J. Am. Chem. Soc.*, 2006, **128**, 8726.
33 D. Marx, *ChemPhysChem*, 2006, **7**, 1848.
34 J. T. Hynes, *Nature*, 2007, **446**, 270.
35 J. A. Richards, P. E. Whitson and D. H. Evans, *J. Electroanal. Chem.*, 1975, **63**, 311.
36 C. Costentin, C. Louault, M. Robert and J.-M. Savéant, *J. Am. Chem. Soc.*, 2008, **130**, 15817.
37 C. Costentin, C. Louault, M. Robert and J.-M. Savéant, *Proc. Natl. Acad. Sci. U. S. A.*, 2009, **106**, 18143.
38 M. Ye and R. H. Schuler, *J. Phys. Chem.*, 1989, **93**, 1898.
39 W. T. Dixon and D. Murphy, *J. Chem. Soc., Faraday Trans.*, 1976, **72**, 1221.
40 L. I. Krishtalik, *Biochim. Biophys. Acta, Bioenerg.*, 2003, **1604**, 13.
41 C. Costentin, M. Robert and J. M. Savéant, *J. Am. Chem. Soc.*, 2007, **129**, 5870.
42 M. Sjödin, S. Styring, B. Akermark, L. Sun and L. Hammarstrom, *J. Am. Chem. Soc.*, 2000, **122**, 3932.
43 M. Sjödin, S. Styring, H. Wolpher, Y. Xu, L. Sun and L. Hammarstrom, *J. Am. Chem. Soc.*, 2005, **127**, 3855.
44 M. Sjödin, T. Irebo, J. E. Utas, J. Lind, G. Merenyi, B. Akermark and L. Hammarstrom, *J. Am. Chem. Soc.*, 2006, **128**, 13076.
45 T. Irebo, S. Y. Reece, M. Sjodin, D. G. Nocera and L. Hammarstrom, *J. Am. Chem. Soc.*, 2007, **129**, 15462.
46 *Handbook of Chemistry and Physics*, CRC Press, 88th Edn, 2000, pp. 5–76 to 5–78.
47 L. Nadjo and J. M. Savéant, *J. Electroanal. Chem.*, 1973, **48**, 113.
48 J. Bonin, C. Costentin, C. Louault, M. Robert, M. Routier and J.-M. Savéant, *Proc. Natl. Acad. Sci. U. S. A.*, 2010, **107**, 3367.
49 N. Song and D. M. Stanbury, *Inorg. Chem.*, 2008, **47**, 11458.
50 J. M. Savéant, *J. Phys. Chem. C*, 2007, **111**, 2819.
51 C. Costentin, D. H. Evans, M. Robert, J. M. Savéant and P. S. Singh, *J. Am. Chem. Soc.*, 2005, **127**, 12490.
52 P. S. Singh and D. H. Evans, *J. Phys. Chem. B*, 2006, **110**, 637.
53 C. A. Wraight, *Biochim. Biophys. Acta, Bioenerg.*, 2006, **1757**, 886.
54 C. Costentin, M. Robert, J. M. Savéant and C. Tard, *Angew. Chem. Intern. Ed.*, in press.